9-2015

The Effect of Scan Settings on the Identification of Tooth Socket Lamina Dura Surface: A CBCT Study

Erick Carlucci

LOMA LINDA UNIVERSITY
School of Dentistry
in conjunction with the
Faculty of Graduate Studies

The Effect of Scan Settings on the Identification of Tooth Socket Lamina Dura Surface: A CBCT Study

by

Erick Carlucci

A thesis submitted in partial satisfaction of
the requirements for the degree
Master of Science in Orthodontics and Dentofacial Orthopedics

---

September 2015

Each person whose signature appears below certifies that this thesis in his/her opinion is adequate, in scope and quality, as a thesis for the degree of Master of Science.

_____, Chairperson
Kitichai Rungcharassaeng, Professor of Orthodontics and Dentofacial Orthopedics

_____
Joseph M. Caruso, Professor of Orthodontics and Dentofacial Orthopedics

_____
Joseph Y.K. Kan, Professor of Restorative Dentistry

ACKNOWLEDGEMENTS

My sincerest gratitude belongs to the members of my research committee and the faculty involved in completing this last phase of my educational journey. I especially appreciate the time, patience, and dedication of Dr. Kitichai Rungcharassaeng, who helped guide and shape this project from start to finish. Secondly, I thank Dr. Joseph Caruso for his profound insight with CBCT. Finally, I want to thank Dr. Joseph Kan for his invaluable advice in developing the project.

Most importantly, I am forever grateful for my amazing family and friends. They, individually and collectively, provide me with more opportunity, support, and love than I deserve. Everything I am and all that I accomplish, I owe to them.

CONTENTS

TABLES

Tables Page

FIGURES

Figures Page

ABBREVIATIONS

CBCT	Cone-Beam Computed Tomography
DAP	Dose-Area Product
FBM	Facial Bone Margin
FBS	Facial Bone Surface
FBT	Facial Bone Thickness
FLD	Facial Lamina Dura
FOV	Field of View
Gp	Group
GxTy	Group-Time-point Combination
Px	Pixel
T1	Time-point 1 (before extraction)
T2	Time-point 2 (after extraction)

ABSTRACT OF THE THESIS

The Effect of Scan Settings on Identification of Tooth Socket Lamina Dura Surface: A CBCT Study

by

Erick Carlucci

Master of Science in Orthodontics and Dentofacial Orthopedics
Loma Linda University, September 2015
Dr. Kitichai Rungcharassaeng, Chairperson

Aim: Cone-beam computed tomography (CBCT) is becoming a common adjunct in orthodontic diagnosis and treatment, however several questions remain about the impact of surrounding anatomical structures and varying scan settings on the ability to delineate buccal bone and overall diagnostic quality of images produced. The aim of this study was to determine if adjacent structures with similar radiodensity and variable scan settings (field of view and voxel size) significantly impact the ability to accurately identify the tooth socket facial lamina dura, facial bone surface, facial bone margin, as well as the facial bone thickness measurement. **Materials & Methods:** CBCT scans (NewTom 5G) were performed on 2 fresh cadaver heads at 2 different time points, before (T1) and after (T2) tooth extraction, using 4 different scan settings that produced images in the decreasing order of clarity: 12x8 cm^2 FOV at 100 µm voxel size (Group 1), 12x8 cm^2 FOV at 150 µm voxel size (Group 2), 18x16 cm^2 FOV at 150 µm voxel size (Group 3), and 18x16 cm^2 FOV at 300µm voxel size (Group 4). The CBCT volumes were superimposed (Invivo 5.2) in pairs, before and after extraction, among the different scan settings (groups). Mid-sagittal images of the teeth were created and eleven total points along the external cortical border and facial lamina dura surface of each socket were

identified. Absolute discrepancies between each pair were recorded and comparisons made using Wilcoxon Signed Rank Tests and Friedman's Two-Way ANOVA ($\alpha = 0.05$). **Results:** Although there were statistically significant differences ($p < 0.05$) in group and time-point discrepancies in 15 of 52 comparisons evaluated, the measured differences were low and likely clinically negligible. **Conclusions:** This study, with its own limitations, shows that the ability to accurately outline buccal bone, irrespective of the presence of the tooth structure, is not clinically significantly affected by the variation in FOV and voxel size of the CBCT images.

CHAPTER ONE

REVIEW OF THE LITERATURE

Cone beam computed tomography (CBCT) is a relatively new imaging technology used to create 3-dimensional renditions of subjects.[1] Following the commercial introduction of CBCT, unprecedented abilities to maxillofacial imaging emerged, immensely expanding the role of imaging within diagnostics and treatment.[1] The benefits of good image quality, volumetric analysis, short scan times, and relatively less radiation dose than conventional medical CT, has resulted in greater ubiquity as an imaging modality within all disciplines of dentistry. Many fields, including orthodontics, oral surgery, implant dentistry, periodontics, and endodontics find unique utility of the 3-dimensional reconstructions provided by CBCT.[3,4] It has become an important adjunct in orthodontic diagnosis due in part to the diverse image reconstructions available (cephalometrics, TMJ cross-sections, etc.), the ability to visualize bony levels, and the sub-millimeter accuracy enabling linear measurements.[2,9]

However, CBCT is known to have shortcomings, such as capturing thin areas of bone.[13,17,22] The accurate imaging of these fine anatomical structures is important to the orthodontic clinician for both initial diagnostic decisions and outcome assessment as the radiographic interpretation of bone levels is often used to determine periodontal health or externalities as the result of treatment. [3,4,19]

There are many components of CBCT image production; the various factors, such as the scanning unit employed, examined object, FOV, contrast resolution, and spatial resolution defined by the voxel size may profoundly influence the image quality produced for interpretation.[5] It is important to understand these details in order to pursue

improvement in the modality on a clinical level. The immediately following paragraphs will elaborate on this detail to establish the foundation for discussion of the scientific study of these variables, and how manipulation will produce different clinical results.

Imaging from the CBCT is accomplished via a rotating gantry, from which a pyramidal x-ray beam is directed through the subject onto a contralateral sensor.[1] The gantry will rotate around the subject simultaneously collecting multiple (from 150 to more than 600), sequential, full-volume, planar projection (2D) images within an assigned field of view (FOV), each individually known as basis images.[1] These basis images are used to mathematically reconstruct the 3-dimensional volume for viewing and manipulation.[1]

With the collection of each individual image in CBCT geometry, the full volume of the subject is scanned, generating a significant amount of omnidirectional scatter that is ultimately recorded by the receptor.[1] This reduces image contrast and increases image noise.[9] The larger the area, or field of view, of the scan, the more scatter generated. The fields of view imaged by CBCT are adjustable and collimation of the x-ray beam limits exposure to the region of interest, allowing the operator to narrow the scope of the image for each individual patient and clinical need.[1] Naturally, the larger fields of view are associated with larger amounts of exposure.[8]

Contrast resolution refers to the ability of an observer to distinguish between two objects of different radiographic densities.[12] High contrast between the margins of an object and surrounding structures improves the observer ability to identify those boundaries at the interface.[9,12] Therefore, the narrow interface between tooth structure

and the enveloping bone, with similar radiodensities, would be more difficult to distinguish than that between air and bone.[9,12]

Spatial resolution is the minimum distance necessary to distinguish between two objects.[9] With CBCT-derived images, spatial resolution, and therefore detail, is primarily defined by individual volume elements or, voxels.[1] A voxel is the 3D equivalent to the 2D pixel, whereby a voxel is defined by its height, width, and depth.[5] CBCT voxels are generally isotropic, meaning equal in all dimensions.[5] The area detector resolution of CBCT units are sub-millimeter, ranging from 0.09 to 0.40mm, principally determining the size of the voxels.[1] Reducing the voxel size during a scan will improve the resolution, at a cost of increased radiation exposure to the patient.[9,20] Thus, the voxel dimension utilized is directly related to the radiation dose to which the patient is submitted during the scan.[17]

There are numerous clinical benefits of the CBCT imaging modality. Rapid scan times result in fewer artifacts due to patient movement.[1] Adjustable FOV adds usage versatility and reduces radiation to the patient.[1] The images produced have sub-millimeter resolutions, allowing for measurement precision.[1] Effective radiation dose to the patient (ranging from 29-477 μSv) relative to traditional medical CT (approximately 2000 μSv) is greatly reduced.[1,21] Multiple, interactive display renditions developed for unique diagnostic and operative clinical needs allow prodigious clinical flexibility.[1]

Current CBCT technology has limitations related to the ‘‘cone-beam’’ projection geometry, detector sensitivity, and contrast resolution that produce images lacking in maximum clarity.[1] The images are subject to artifacts, noise, and poor soft tissue contrast.[1] Study and development of the technology aims to mitigate the present

shortcomings, achieving images that most accurately and flawlessly represent the anatomical truth.

A considerably large amount of factors are integral to the production of CBCT volumes.[9] This intricate and multifactorial nature of CBCT image production raises many questions. Operationally adjustable parameters such as FOV and spatial resolution (voxel size) change the diagnostic outcome of CBCT generated images.[5] However, the consequences, the magnitude of those consequences, and the appropriate clinical applications are all poorly understood. For medical CT examinations, settings or protocols for any application are well established.[5] Conversely, rationales for standardized protocols and their impact on CBCT-based diagnosis are presently unavailable for dentistry.[5] This is important for the clinician to judiciously utilize CBCT technology, adhering to the ALARA principle of maximizing clinical benefit to the patient and minimizing the risks inherent to ionizing radiation.[6-8]

Many studies exist, employing a diverse variety of methodologies that demonstrate the ability of CBCT to produce accurate images. Initial reporting on accuracy began in 2004, with two notable publications by Kobayashi et al and Lascala et al.[10,11] Kobayashi used cadaver mandibles and Lascala used dry skulls, each comparing actual measurements to those made on CBCT, concluding that it is reliable for linear measurements of structures closely associated with dentomaxillofacial imaging.[10,11]

Studies began to manipulate scanning parameters such as FOV and voxel size, in order to evaluate the outcome on image quality. In early 2010, Damstra et al used dry mandibles embedded with glass spheres to evaluate the linear accuracy of CBCT generated surface models with 2 different voxel sizes (0.40mm and 0.25mm) and

concluded accuracy in the CBCT measurement procedure with no significant difference between the voxel resolutions.[15] An inherent, and acknowledged, limitation in this study was the lack of soft tissues, resulting in increased contrast of the landmarks, influencing the outcome.[15]

With demonstrable accuracy over long distances, investigation in the limits of spatial resolution emerged. Sun et al used pig specimens to measure alveolar bone height from CBCT generated images with varying voxel sizes.[12] These authors found evidence that decreasing voxel size improved the accuracy of alveolar bone measurements.[12] In an effort to most closely emulate a clinical setting, Patcas et al used intact cadaver heads and evaluated the ability of CBCT, with varying voxel resolutions, to detect the bony covering of mandibular anterior teeth.[13] Differing in conclusions by Damstra regarding the significance of voxel resolutions, Patcas' results, along with the earlier report by Sun et al,[12] suggest demonstrated improvement in accuracy when decreasing the voxel size.[13] Despite that improvement however, the authors went on to discuss that differences between clinical and radiographic measurements can be as large as 2mm, showing that the average alveolar bone thickness of 1mm might be missed completely.[13] Overall, this report concluded that CBCT is an appropriate tool for linear measurements and that the presence of surrounding tissue as well as different voxel size affect the precision of the data.[13] It was acknowledged that even the most granular 0.125-mm voxel protocol does not depict the thin buccal alveolar bone covering reliably, resulting in a risk of overestimating fenestrations and dehiscences.[13] This unreliability is substantiated by Leung et al., who found that CBCT has a high rate of false positives with 3 times the

number of fenestrations detected than existed in reality and a significant number of false negatives with more than half of real dehiscences undetected.[22]

In an article recently published by Cook et al, the authors varied scanning parameters and measured buccal alveolar bone height and thickness on human cadavers. Their protocol compared images generated from a "long scan" with 619 basis images, 360° revolution, 26.9s duration, and 0.2mm voxel size against those from a "short scan" with 169 basis images, 180 rotation, 4.8s duration, and 0.3mm voxel size; the measurements made from these scans were compared to direct caliper measurement.[14] The authors found no statistically significant differences between these parameter changes and concluded that the parameters resulting in a lower radiation dose to the patient was favorable unless the need for the higher resolution could be clearly defined.[14]

Studies with variations in voxel size during analysis extend beyond the evaluation of bone landmarks and measurement. A systematic review conducted by Spin-Neto et al collated 20 different publications which qualitatively or quantitatively assessed the influence of voxel size on CBCT-based diagnostic outcome.[5] The diagnostic tasks evaluated in the studies included in the review were diverse, including detection of root fractures, detection of external root resorption, caries detection, and accuracy bony measurements, among others.[5] Some of the included studies demonstrated improvement in image quality and diagnostic accuracy, while others presented no difference.[5,15,16,23-27] Aggregately, the studies dealing with categorical data showed a tendency towards more accurate results associated with higher voxel resolutions.[5] However, Spin-Neto concluded that it is not yet possible to propose general protocols for the myriad of diagnostic applications with CBCT.[5] With the lack of unanimity, all of these

investigations emphasize the need for a better understanding of the factors that influence image resolution with current CBCT technology.

Many authors have further discussed a concept referred to as the partial volume averaging effect.[1,5,9,12] This effect is a cone beam related artifact in which, depending on the voxel size, radiopaque structures could become invisible. As defined by Scarfe and Farman, partial volume averaging occurs when the selected voxel resolution of the scan is greater than the spatial or contrast resolution of the object to be imaged.[1] Meaning, the voxel is larger than the anatomical structure imaged and captures the image of two objects of different radiodensities. This voxel will then render the average density of both objects rather than the true density of either object.[5] Selection of the smallest acquisition voxel can reduce the effect of this averaging.[1] Known limitations in contrast resolution associated with CBCT units could also contribute to the invisibility of structures with similar radiodensities in close proximity.[5,12] The deficiencies as a result of low contrast resolution and partial volume averaging acknowledged by many authors are important to understand, and are critical concepts in future CBCT research.

Although CBCT has a relatively lower radiation dose to patients than medical CT, practitioners must be prudent in prescribing imaging in adherence to the ALARA principle (radiation dose 'as low as reasonably achievable'). A myriad of factors contribute to the radiation exposure, among which are the aforementioned user adjustable settings of voxel size and FOV.[1,8] Other factors include scan duration, milliamperage, kilovolt potential, filtering, patient positioning, and the sensor technology and proprietary algorithms used in the device itself.[1] All of this makes CBCT dosimetry inherently difficult to summarize.[8] To further obfuscate, much of the research available relies on

different methodologies and comparisons to draw conclusions about radiation exposure. DeVoss et al conducted a systematic review of CBCT in 2009 and discussed findings on radiation dose in the literature. These authors found inconsistencies in how CBCT device settings, properties, and radiation dose were reported; all contributing to reader confusion.[28] They stated the importance of rigorous and consistent reporting on the different relevant parameters and acquisition protocols since device settings, image quality, and the resulting radiation exposure are closely related.[28] In 2013, Rottke et al studied the effective dose (ED) span of ten different commercially available CBCT devices.[21] Performing protocols with the lowest exposition parameters and protocols with the highest exposition protocols for each of the ten devices, they found a wide range of EDs.[21] The average value for the protocols with the lowest exposition parameters was 31.6 μSv and 209 μSv for protocols with the highest exposition parameters.[21] The aim of that study was limited to dosimetry, so the quality of these images were not addressed.[21] However, they did acknowledge that some of the volumes could be of no diagnostic use due to such poor image quality.[21]

The underscored principle of utilizing CBCT for diagnosis and treatment planning in dentistry is maximizing the clinical benefit for the patient while minimizing the risks of ionizing radiation. The CBCT modality offers diverse utility but should be used prudently with the relationship between dose and image quality carefully considered.[6-8] It is evident that the scan parameters are significant to both of these.[5,8] With all of its diverse uses and technical variability, dentistry has yet to develop standardized CBCT examination protocols.[5-7]

A more detailed understanding of the impact that differing scan settings have on the ability to discern fine anatomic structures will enable the practitioner to better and more judiciously examine patients and elevate the profession's comprehension and confidence in this instrument. The objective of this research is to determine if variable scan settings, specifically field of view and voxel size, significantly impact the ability to accurately outline the buccal bone surfaces. The null hypothesis was that no differences would be observed. The alternative hypothesis was that the varying settings would significantly affect the resolution of the images produced and subsequently the diagnostic quality.

CHAPTER TWO

THE EFFECT OF SCAN SETTINGS ON IDENTIFICATION OF TOOTH SOCKET LAMINA DURA: A CBCT STUDY

Abstract

Aim: Cone-beam computed tomography (CBCT) is becoming a common adjunct in orthodontic diagnosis and treatment, however several questions remain about the impact of surrounding anatomical structures and varying scan settings on the ability to delineate buccal bone and overall diagnostic quality of images produced. The aim of this study was to determine if adjacent structures with similar radiodensity and variable scan settings (field of view and voxel size) significantly impact the ability to accurately identify the tooth socket facial lamina dura, facial bone surface, facial bone margin, as well as the facial bone thickness measurement. **Materials & Methods:** CBCT scans (NewTom 5G) were performed on 2 fresh cadaver heads at 2 different time points, before (T1) and after (T2) tooth extraction, using 4 different scan settings that produced images in the decreasing order of clarity: 12x8 cm^2 FOV at 100 µm voxel size (Group 1), 12x8 cm^2 FOV at 150 µm voxel size (Group 2), 18x16 cm^2 FOV at 150 µm voxel size (Group 3), and 18x16 cm^2 FOV at 300µm voxel size (Group 4). The CBCT volumes were superimposed (Invivo 5.2) in pairs, before and after extraction, among the different scan settings (groups). Mid-sagittal images of the teeth were created and eleven total points along the external cortical border and facial lamina dura surface of each socket were identified. Absolute discrepancies between each pair were recorded and comparisons made using Wilcoxon Signed Rank Tests and Friedman's Two-Way ANOVA ($\alpha = 0.05$). **Results:** Although there were statistically significant differences ($p < 0.05$) in group and

time-point discrepancies in 15 of 52 comparisons evaluated, the measured differences were low and likely clinically negligible. **Conclusions:** This study, with its own limitations, shows that the ability to accurately outline buccal bone, irrespective of the presence of the tooth structure, is not clinically significantly affected by the variation in FOV and voxel size of the CBCT images.

Introduction

Cone beam Computed Tomography (CBCT) is acclaimed for its accuracy and diverse clinical utility.[1] The benefits of good image quality, volumetric analysis, short scan times, and relatively less radiation dose than conventional medical CT, has resulted in greater ubiquity as an imaging modality within all disciplines of dentistry.[1] It has become an important adjunct in orthodontic diagnosis due in part to the diverse image reconstructions available (cephalometrics, TMJ cross-sections, etc.), the ability to visualize bony levels, and the sub-millimeter accuracy enabling linear measurements.[2] In particular, evaluating fine anatomical structures, like alveolar bone enveloping teeth, is important to the orthodontist for both initial diagnostic knowledge and outcome assessment.[3] The ability to characterize buccal bone has clear benefits for practitioners in periodontics and implant dentistry as well.[4]

There are many components of CBCT image production. The various factors, such as the scanning unit employed, examined object, FOV, and spatial resolution defined by the voxel size may profoundly influence the image quality produced for interpretation.[5] However, the consequences, the magnitude of those consequences, and the appropriate clinical applications are not well understood.

Moreover, the fundamental principle of utilizing CBCT for diagnosis and treatment planning in dentistry is to maximize the clinical benefit for the patient while minimizing the risks of ionizing radiation.[6-8] The CBCT modality offers diverse utility but should be used prudently with the relationship between dose and image quality carefully considered.[6-8] It is evident that the adjustable voxel size and FOV scanning parameters are significant to both of these.[5,7,8] With all of its diverse uses and technical

variability, dentistry has yet to develop standardized CBCT examination protocols.[5,6,8] The development of these protocols would help guide practitioners when prescribing this modality for the wide variety of clinical applications.[5]

The objective of this research is to determine if variable scan settings, specifically field of view and voxel size, significantly impact the ability to accurately outline the buccal bone surfaces. The null hypothesis was that no differences would be observed. The alternative hypothesis was that the varying settings would significantly affect the resolution of the images produced and subsequently the diagnostic quality.

Materials and Methods

Two fresh, frozen, dentate cadaver heads were obtained from the Loma Linda University Bodies for Science program. The study was filed but exempted from IRB approval. The heads were first screened using the following criteria:

1. Each head must contain as many teeth as possible, with a minimum of 10 teeth per jaw, which must include at least one molar bilaterally.
2. As few metallic restorations as possible.
3. No or minimal periodontal destruction.
4. No visible structural damage resulting from trauma or pathology in either jaw.

Impressions were made of each arch using irreversible hydrocolloid impression material (Dust-Free Fast-Set Alginate, Dux Dental, California) and casts were fabricated using dental stone (Ortho Stone, Heraus-Kulzer Inc., Germany). Block-out resin (LC Block-out Resin, Ultradent, Missouri) was used to eliminate undercuts on the casts.

A radiographic template was then constructed of 2 mm vacuum-formed plastic (Splint Bioacryl, Great Lakes Orthodontics, New York). Radiopaque 2-3 mm pieces of 18 gauge aluminum wire (Impex System Collaborators, Florida) were fixed to the template with a radiolucent non-filled resin (Adper Scotchbond Multi-Purpose Adhesive, 3M ESPE, Minnesota) at the incisal tip, the free gingival margin, and the deepest edge of the template (Figures 1, 2). The intent was to use the radiographic template as guide for image superimposition, and it was used in all CBCT scans.

Figure 1: Working model with radiographic template, right oblique view. Aluminum markers are present at the approximate incisal tip, gingival margin, and deepest vestibular margin.

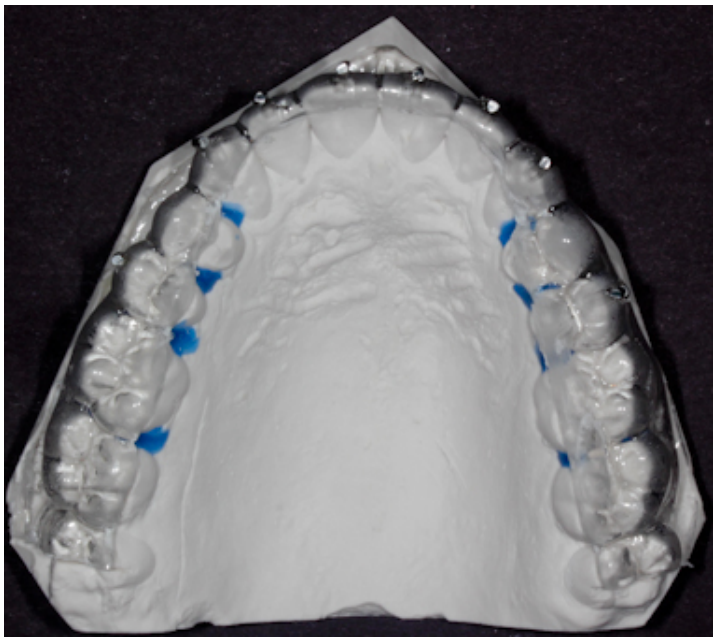

Figure 2: Working model with radiographic template, occlusal view. Note that the plastic envelops the occlusal/incisal surfaces of the teeth for stability.

The scans were performed using a NewTom 5G CBCT device (QR S.r.l., Verona, Italy). Volumes were captured using a total of 4 different scan settings, each employing a distinct combination of different fields of view (FOV, cm x cm) and voxel sizes (VS, µm): 12x8 at 100 (Group 1), 12x8 at 150 (Group 2), 18x16 at 150 (Group 3), and 18x16 at 300 (Group 4) (Table 1). The scans were performed using 110 kVp, with a range of 0.64-14.87 mA (varying according to chosen setting and the size of the head), 5.4 s scan time for the smaller FOV, and a 3.6 s scan time for the larger FOV. Initial scans were performed before any alteration to the teeth or tissues (T1).

Table 1: Group assignments and their respective scan settings.

	Voxel Size (µm)	FOV (cm x cm)
Group 1 (G1)	100	12 x 8
Group 2 (G2)	150	12 x 8
Group 3 (G3)	150	18 x 16
Group 4 (G4)	300	18 x 16

Single rooted teeth were selected for extraction to reduce the potential damage to the surrounding alveolar bone and to minimize the chance of root fracture. First premolars and all existing molars were not extracted and utilized to provide support and stability to the template.

Extractions were performed using a Periotome instrument (Nobel Biocare, Yorba Linda, California), periosteal elevators, and extraction forceps. The supracrestal gingival attachment was carefully severed to preserve the gingiva. Luxation was performed with a Periotome instrument followed by periosteal elevators. The luxated teeth were gently delivered with extraction forceps, the radiographic template was then reseated and the post-extraction scans taken (T2), again according to the parameters of the 4 groups.

Each CBCT volume was labeled according to its group and the time point it was taken (GxTy); for example, Group 1 at T1 is labeled as G1T1, etc. The volumes were superimposed three-dimensionally in pairs (according to the selected time point and scan parameter for comparison) using Invivo software (Anatomage, v.5.2, San Jose, California). Precise superimpositions were generated manually using hard tissue landmarks including cortical borders, medullary trabeculation, and roots of non-extracted teeth (Figure 3). All superimpositions were performed by a single examiner (EC).

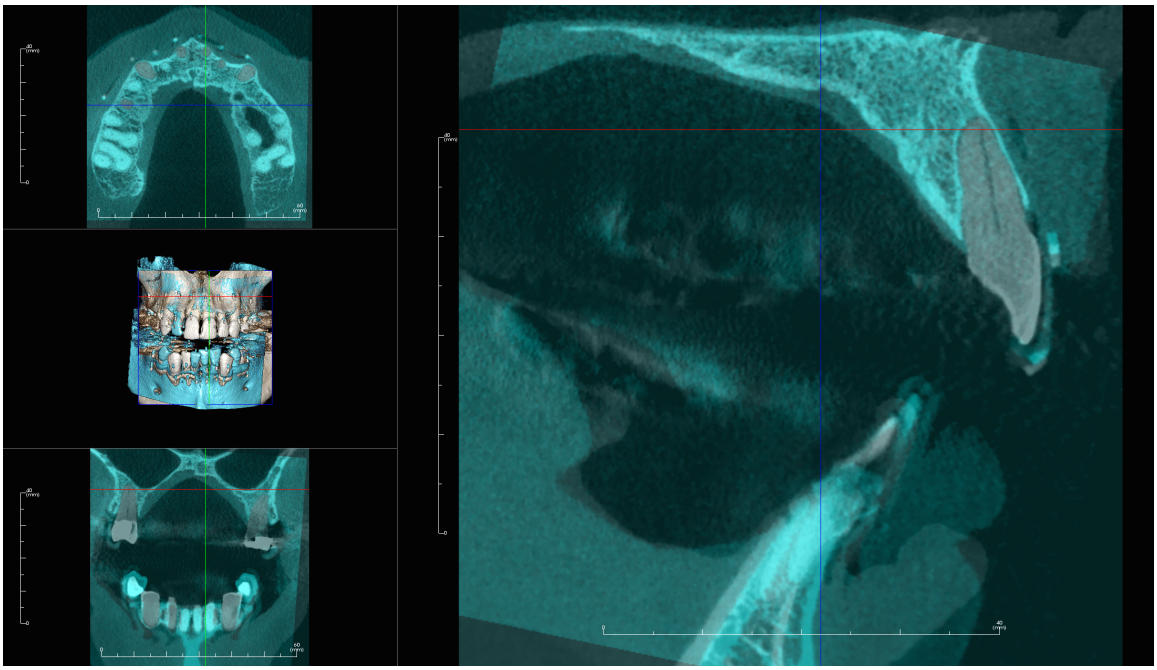

Figure 3: Example of volume superimposition. T1-T2 superimposition of the maxillary right central incisor, MPR with sagittal plane enlarged. Upper and lower jaws were independently superimposed, with bony landmarks prioritized.

The superimposition pairs, made among the 4 different groups and 2 time points, are illustrated by Figure 4. Comparisons among each group and time-point are intended to evaluate interaction effects between these variables. This will reveal which parameter, FOV, VS, or both are contributory to any differences observed.

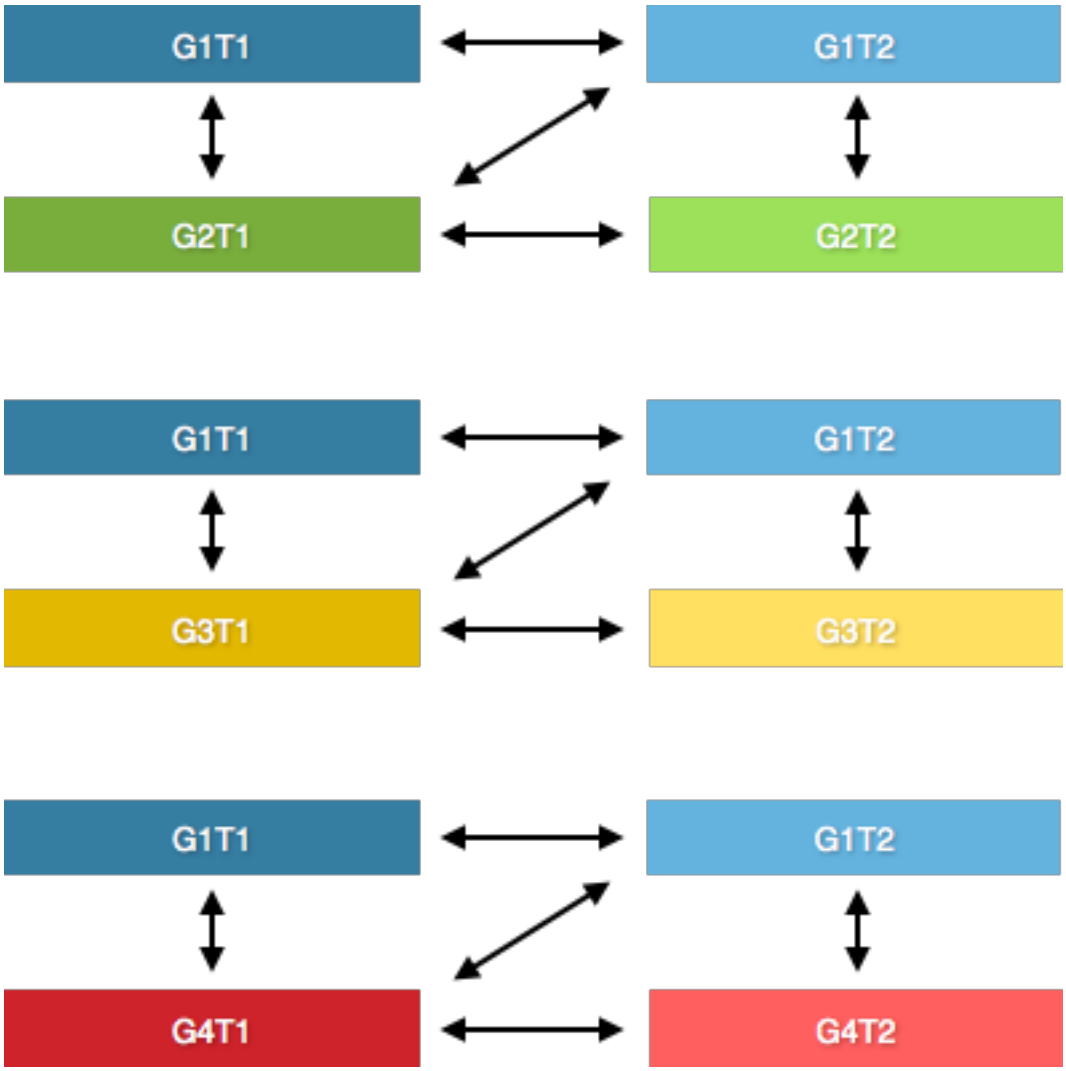

Figure 4: The group-time-point combinations (GxTy) and the superimposition pairs (as denoted by the arrows) for image comparison.

Mid-sagittal images, along the long axis of the tooth, were produced for each superimposition pairing. These images were then screen captured and imported into the Keynote presentation program (v.6.5.3, Apple Inc., California) for analysis as performed in Roe et al.[4] Using a slide resolution of 1024x768, the length of the Anatomage ruler (40 mm) was sized to equate to 400 pixels on the Keynote slide, which translates to 0.1 mm per pixel. A representative sample of 8 created images from a single tooth, corresponding to each group-time-point combination (GxTy) is illustrated in Figure 5. Images of mandibular teeth were vertically inverted in order to preserve consistency with coordinate mapping between maxillary and mandibular teeth. The first paired-image was then rotationally oriented until the line connecting facial and lingual CEJs (CEJ Line) was horizontal. This angular change of the image was recorded and used to orient the remaining paired-images. The X-Y coordinates of the Anatomage rulers on both pair-images should match along with the bony landmarks mentioned above, to ensure no positional discrepancies exist.

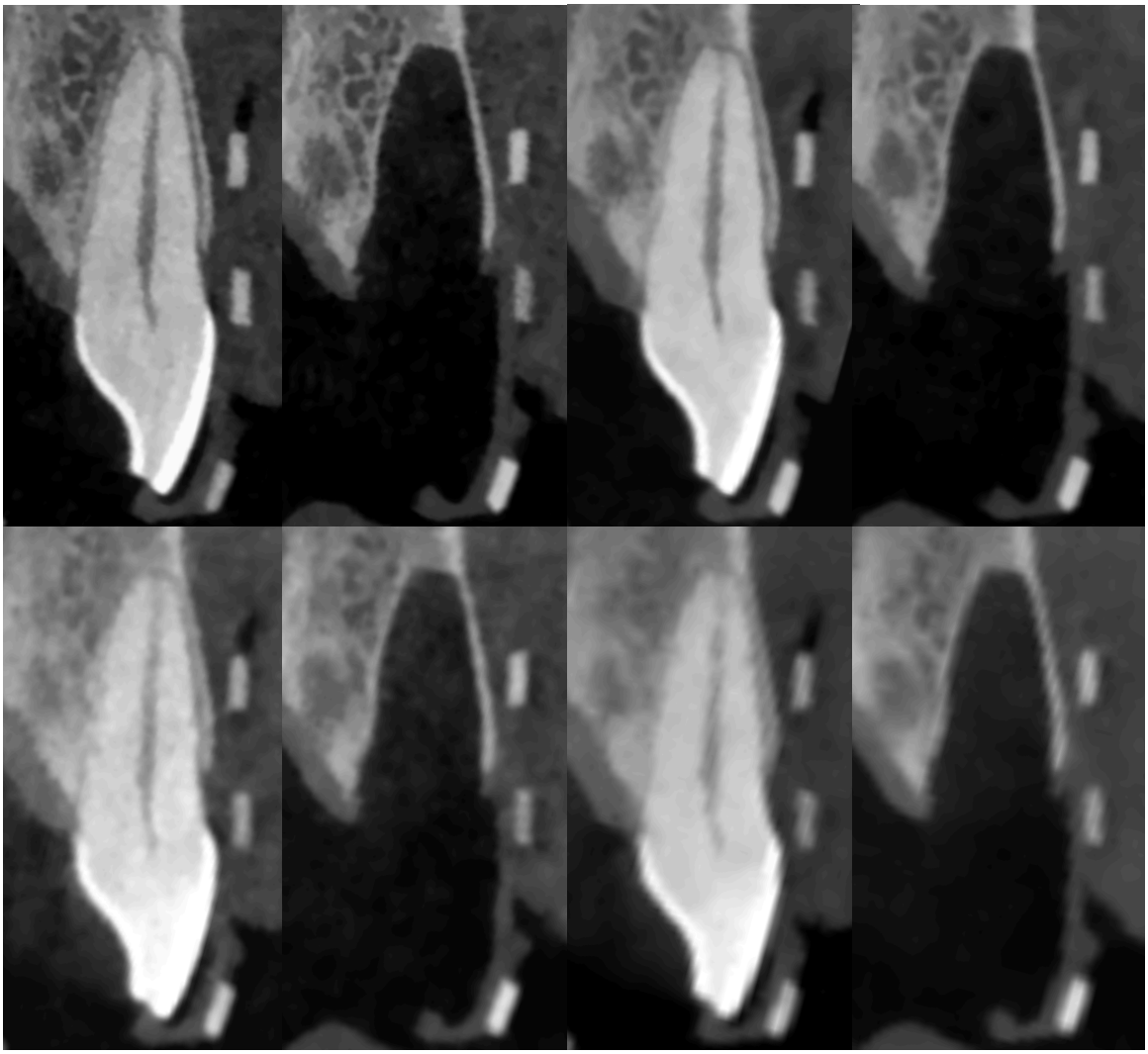

Figure 5: Images of a maxillary central incisor, representing the 8 different group-time-point combinations. From top left to bottom right respectively: GT1T1, GT1T2, GT2T1, GT2T2, GT3T1, GT3T2, GT4T1, GT4T2. The images were captured at exactly the same sagittal slice and imported into Keynote for positioning and coordinate identification.

A grid was superimposed on the images with the following lines: 1) the horizontal CEJ Line, 2) a vertical reference line perpendicular to the CEJ line, and 3) the Level Lines parallel and at 3, 5, 7, 9 and 11 mm apical to the CEJ Line (Level Lines 1-5, respectively; Figure 6). The facial lamina dura (FLD) and facial bone surface (FBS) were identified with single pixel points along the corresponding Level Lines, and the facial bone margin (FBM) is identified with a single pixel point at the crest of the alveolus (Figure 6).

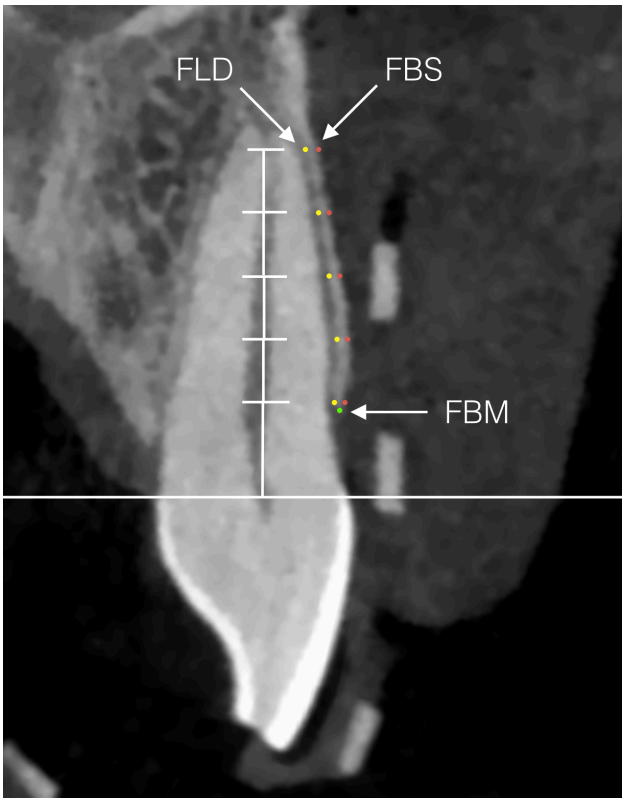

Figure 6: Constructed grid in Keynote presentation program. The image was rotated to match the buccal and lingual CEJs with the horizontal CEJ Line. Landmark identification represented with the colored dots (enlarged for illustrative purposes). The examiner used these dots to plot the FLD (blue), FBS (red), and FBM (green). In cases where the bone margin was >3 mm from the CEJ line, the X-axis points at the 3 mm mark were discarded.

The coordinates were recorded and the group-time-point combination discrepancies calculated in horizontal plane using X-axis coordinates. Facial bone thickness (FBT) at each Level Line is the difference between FBS and FLD X-axis coordinates and expressed in pixels. The facial bone margin (FBM) was also identified, however the discrepancies were calculated in the vertical plane using Y-axis coordinates (Figure 6). Discrepancies in the X-axis were given a positive value when the second time-point moved away from the socket, and a negative value when discrepancies moved toward the socket. Discrepancies in the Y-axis were given a positive value when the second time-point moved coronal, and a negative value when it moved apical. These directional discrepancies were subsequently converted to absolute values and recorded as absolute discrepancies. Figure 7 illustrates the landmark identification (pixel point placements) and visual discrepancies when superimposed. A single examiner (EC) performed all point placements for each tooth and group-time-point combination in Keynote (Figure 6-7), where pixel size remains constant at 0.1 mm. The landmark identifications were performed first on the images with the lower resolutions and teeth present, followed by plotting on each of the incrementally more resolute imagery (i.e. G4T1 before G4T2, followed by G3T1 before G3T2, etc.). Areas with visible damage after luxation/extraction were excluded from the analysis.

During landmark identification, some coordinates were not clearly delineated and required a professional judgment in order to identify. These points were tabulated in order to evaluate the frequency distribution of this occurrence.

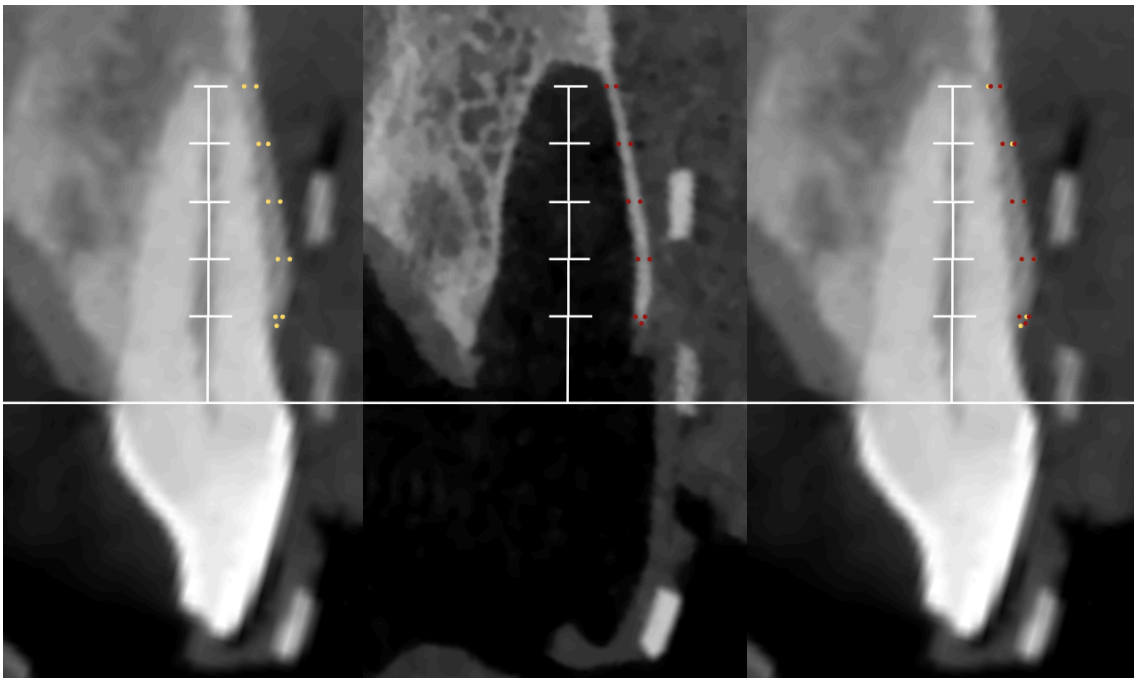

Figure 7: Landmark identification of the representative maxillary central incisor at G4T1 (left), G1T2 (middle), and the two pixel point grids superimposed on the G4T1 image (right). The pixel points above were enlarged for illustrative purposes. The discrepancies in coordinates can be easily visualized. The exact coordinates were recorded and discrepancies calculated for each image.

Statistical Analysis

The intra-examiner reliability of the method was determined by using double assessments of each parameter by examiner EC on the images produced from each GxTy combination from 5 randomly selected teeth made at least 2 weeks apart and expressed as the intraclass correlation coefficients (ICC). Means and standard deviations of both directional and absolute discrepancies were calculated for each parameter. Only absolute discrepancy data were analyzed statistically using Spearman's Rank Correlation analysis, Wilcoxon Signed Rank, and Friedman's Two-Way Analysis of Variance by Ranks Tests. The significance level of $\alpha = 0.05$ was used for all statistical analyses.

Results

A total of 24 (20 maxillary and 18 mandibular) teeth and their respective sockets were evaluated in this study. The tooth distribution is shown in Table 2.

Table 2: List of Extracted Teeth by Head.

Tooth	Head 1	Head 2	Total
Mx Central	2	2	4
Mx Lateral	2	1	3
Mx Canine	1	2	3
Mx 2nd Premolar	1	2	3
Mn Central	2	0	2
Mn Lateral	0	1	1
Mn Canine	2	2	4
Mn 2nd Premolar	2	2	4
Total	12	12	24

ICC values were very high for intra-examiner ($r \geq 0.993$) data, indicating that the identification methods were reliable and reproducible. Tables 3-6 display the means and standard deviations of both directional and absolute discrepancies between different paired GxTy combinations for FLD (Table 3), FBS (Table 4), FBT (Table 5), and FBM (Table 6). The means ranged from -0.11 ± 0.19 mm to 0.10 ± 0.19 mm for directional and 0.05 ± 0.06 mm to 0.24 ± 0.24 mm for absolute discrepancies (Tables 3-6). The identified coordinates between paired GxTy combinations (values not shown) were compared Wilcoxon Signed Rank Tests, and correlated using Spearman's Rho at $\alpha = 0.05$. Statistically significant differences were found for the Facial Lamina Dura (7 pairs), Facial Bone Surface (3 pairs), and Facial Bone Thickness (5 pairs) [$p < .05$; Tables

3-5]. No significant differences were found for the Facial Bone Margin ($p > .05$; Table 6).

All paired coordinates were highly correlated ($r > 0.883$, $p < 0.001$; Tables 3-6).

Table 3: Directional and absolute discrepancies between paired GxTy combinations for the Facial Lamina Dura parameter (N=96). Pairwise comparisons made using Wilcoxon Signed Rank Test, and correlated using Spearman's Rho at $\alpha = 0.05$.

	Paired GxTy Discrepancy				
	Mean ± SD in mm (min-max)		Wilcoxon	Spearman's Rho	
Paired GxTy	Directional Δ	Absolute Δ	p-value	r-value	p-value
G1T1 v G1T2	−0.05 ± 0.13 (−0.5 - 0.3)	0.09 ± 0.11 (0.0 - 0.5)	.087	1	<.001
G1T1 v G2T1	0.04 ± 0.09 (−0.1 - 0.3)	0.06 ± 0.07 (0.0 - 0.3)	.166	1	<.001
G1T1 v G3T1	0.07 ± 0.11 (−0.4 - 0.3)	0.09 ± 0.09 (0.0 - 0.4)	<.001*	1	<.001
G1T1 v G4T1	0.10 ± 0.13 (−0.2 - 0.5)	0.13 ± 0.11 (0.0 - 0.5)	<.001*	1	<.001
G1T2 v G2T1	−0.01 ± 0.17 (−0.5 - 0.5)	0.12 ± 0.12 (0.0 - 0.5)	1	0.999	<.001
G1T2 v G2T2	−0.01 ± 0.08 (−0.2 - 0.3)	0.05 ± 0.06 (0.0 - 0.3)	1	1	<.001
G1T2 v G3T1	0.04 ± 0.18 (−0.5 - 0.4)	0.14 ± 0.12 (0.0 - 0.5)	.577	0.999	<.001
G1T2 v G3T2	0.03 ± 0.10 (−0.2 - 0.3)	0.08 ± 0.07 (0.0 - 0.3)	.742	1	<.001
G1T2 v G4T1	0.10 ± 0.19 (−0.5 - 0.5)	0.17 ± 0.13 (0.0 - 0.5)	<.001*	0.999	<.001
G1T2 v G4T2	0.05 ± 0.13 (−0.6 - 0.3)	0.10 ± 0.10 (0.0 - 0.6)	.014*	1	<.001
G2T1 v G2T2	0.04 ± 0.12 (−0.4 - 0.4)	0.09 ± 0.09 (0.0 - 0.4)	.003*	1	<.001
G3T1 v G3T2	0.04 ± 0.16 (−0.4 - 0.4)	0.12 ± 0.11 (0.0 - 0.4)	.012*	0.999	<.001
G4T1 v G4T2	0.08 ± 0.15 (−0.3 - 0.5)	0.13 ± 0.11 (0.0 - 0.5)	<0.001*	0.999	<0.001

*Statistically significant difference.

Table 4: Directional and absolute discrepancies between paired GxTy combinations for the Facial Bone Surface parameter (N=96). Pairwise comparisons made using Wilcoxon Signed Rank Test, and correlated using Spearman's Rho at $\alpha = 0.05$.

	Paired GxTy Discrepancy				
	Mean ± SD in mm (min-max)		Wilcoxon	Spearman's Rho	
Paired GxTy	Directional Δ	Absolute Δ	p-value	r-value	p-value
G1T1 v G1T2	0.02 ± 0.11 (−0.4 - 0.3)	0.06 ± 0.09 (0.0 - 0.4)	.645	1	<.001
G1T1 v G2T1	0.03 ± 0.08 (−0.1 - 0.4)	0.05 ± 0.07 (0.0 - 0.4)	.338	1	<.001
G1T1 v G3T1	0.03 ± 0.11 (−0.2 - 0.4)	0.07 ± 0.09 (0.0 - 0.4)	1	0.999	<.001
G1T1 v G4T1	−0.01 ± 0.16 (−0.6 - 0.4)	0.10 ± 0.12 (0.0 - 0.6)	1	0.999	<.001
G1T2 v G2T1	0.04 ± 0.12 (−0.2 - 0.4)	0.08 ± 0.09 (0.0 - 0.4)	.577	0.999	<.001
G1T2 v G2T2	0.00 ± 0.10 (−0.2 - 0.3)	0.06 ± 0.07 (0.0 - 0.3)	1	0.999	<.001
G1T2 v G3T1	0.02 ± 0.13 (−0.3 - 0.4)	0.10 ± 0.09 (0.0 - 0.4)	1	0.999	<.001
G1T2 v G3T2	0.01 ± 0.11 (−0.2 - 0.3)	0.08 ± 0.07 (0.0 - 0.3)	1	1	<.001
G1T2 v G4T1	0.03 ± 0.17 (−0.4 - 0.4)	0.13 ± 0.11 (0.0 - 0.4)	1	0.999	<.001
G1T2 v G4T2	0.04 ± 0.13 (−0.3 - 0.4)	0.11 ± 0.09 (0.0 - 0.4)	.055	1	<.001
G2T1 v G2T2	0.04 ± 0.11 (−0.3 - 0.4)	0.08 ± 0.08 (0.0 - 0.4)	<.001*	1	<.001
G3T1 v G3T2	0.05 ± 0.15 (−0.7 - 0.4)	0.11 ± 0.11 (0.0 - 0.7)	<.001*	1	<.001
G4T1 v G4T2	0.08 ± 0.13 (−0.3 - 0.5)	0.11 ± 0.11 (0.0 - 0.5)	<.001*	1	<.001

* Statistically significant difference.

Table 5: Directional and absolute discrepancies between paired GxTy combinations for the Facial Bone Thickness parameter (N=96). Pairwise comparisons made using Wilcoxon Signed Rank Test, and correlated using Spearman's Rho at $\alpha = 0.05$.

	Paired GxTy Discrepancy				
	Mean ± SD in mm (min-max)		Wilcoxon	Spearman's Rho	
Paired GxTy	Directional Δ	Absolute Δ	p-value	r-value	p-value
G1T1 v G1T2	0.07 ± 0.13 (−0.4 - 0.5)	0.10 ± 0.11 (0.0 - 0.5)	<.001*	0.939	<.001
G1T1 v G2T1	−0.01 ± 0.10 (−0.2 - 0.4)	0.06 ± 0.08 (0.0 - 0.4)	1	0.968	<.001
G1T1 v G3T1	−0.05 ± 0.13 (−0.4 - 0.4)	0.10 ± 0.09 (0.0 - 0.4)	.01*	0.949	<.001
G1T1 v G4T1	−0.11 ± 0.19 (−0.8 - 0.4)	0.16 ± 0.15 (0.0 - 0.8)	<.001*	0.928	<.001
G1T2 v G2T1	0.05 ± 0.16 (−0.5 - 0.6)	0.11 ± 0.13 (0.0 - 0.6)	.805	0.917	<.001
G1T2 v G2T2	0.01 ± 0.12 (−0.3 - 0.4)	0.08 ± 0.08 (0.0 - 0.4)	1	0.946	<.001
G1T2 v G3T1	−0.02 ± 0.18 (−0.5 - 0.5)	0.13 ± 0.12 (0.0 - 0.5)	1	0.924	<.001
G1T2 v G3T2	−0.02 ± 0.12 (−0.3 - 0.4)	0.09 ± 0.08 (0.0 - 0.4)	1	0.946	<.001
G1T2 v G4T1	−0.06 ± 0.20 (−0.7 - 0.7)	0.16 ± 0.14 (0.0 - 0.7)	.044*	0.917	<.001
G1T2 v G4T2	−0.09 ± 0.18 (−0.5 - 0.5)	0.16 ± 0.12 (0.0 - 0.5)	<.001*	0.932	<.001
G2T1 v G2T2	0.01 ± 0.15 (−0.5 - 0.4)	0.10 ± 0.10 (0.0 - 0.5)	.326	0.923	<.001
G3T1 v G3T2	0.01 ± 0.21 (−0.9 - 0.5)	0.14 ± 0.15 (0.0 - 0.9)	.259	0.883	<.001
G4T1 v G4T2	−0.01 ± 0.18 (−0.5 - 0.5)	0.13 ± 0.12 (0.0 - 0.5)	.797	0.940	<.001

* Statistically significant difference.

Table 6: Directional and absolute discrepancies between paired GxTy combinations for the Facial Bone Margin parameter (N=24). Pairwise comparisons made using Wilcoxon Signed Rank Test, and correlated using Spearman's Rho at $\alpha = 0.05$.

	Paired GxTy Discrepancy				
	Mean ± SD in mm (min-max)		Wilcoxon	Spearman's Rho	
Paired GxTy	Directional Δ	Absolute Δ	p-value	r-value	p-value
G1T1 v G1T2	0.07 ± 0.20 (−0.3 - 0.8)	0.12 ± 0.18 (0.0 - 0.8)	.122	0.999	<.001
G1T1 v G2T1	0.00 ± 0.13 (−0.3 - 0.3)	0.08 ± 0.10 (0.0 - 0.3)	.952	0.999	<.001
G1T1 v G3T1	−0.06 ± 0.37 (−1.7 - 0.2)	0.16 ± 0.34 (0.0 - 1.7)	.984	0.997	<.001
G1T1 v G4T1	−0.08 ± 0.35 (−1.5 - 0.2)	0.16 ± 0.33 (0.0 - 1.5)	.490	0.996	<.001
G1T2 v G2T1	0.05 ± 0.14 (−0.2 - 0.3)	0.12 ± 0.09 (0.0 - 0.3)	.087	0.997	<.001
G1T2 v G2T2	0.02 ± 0.16 (−0.3 - 0.4)	0.13 ± 0.10 (0.0 - 0.4)	.624	0.997	<.001
G1T2 v G3T1	0.03 ± 0.28 (−0.5 - 0.9)	0.18 ± 0.21 (0.0 - 0.9)	.787	0.997	<.001
G1T2 v G3T2	0.02 ± 0.17 (−0.3 - 0.3)	0.14 ± 0.11 (0.0 - 0.3)	.535	0.997	<.001
G1T2 v G4T1	−0.05 ± 0.21 (−0.7 - 0.2)	0.14 ± 0.17 (0.0 - 0.7)	.596	0.996	<.001
G1T2 v G4T2	0.05 ± 0.24 (−0.6 - 0.4)	0.19 ± 0.15 (0.0 - 0.6)	.184	0.997	<.001
G2T1 v G2T2	0.09 ± 0.26 (−0.4 - 0.8)	0.17 ± 0.21 (0.0 - 0.8)	.113	0.998	<.001
G3T1 v G3T2	0.04 ± 0.34 (−0.8 - 0.8)	0.24 ± 0.24 (0.0 - 0.8)	.388	0.993	<.001
G4T1 v G4T2	0.08 ± 0.27 (−0.4 - 0.8)	0.18 ± 0.22 (0.0 - 0.8)	.284	0.999	<.001

Tables 7-10 depict the comparison of the absolute discrepancies (discrepancies) between paired GxTy combinations for all parameters using Friedman's Two-Way Analysis of Variance by Ranks and Wilcoxon Signed Rank Tests with Bonferroni adjustment for pairwise comparisons at $\alpha = 0.05$.

Table 7 compares the absolute discrepancies between time-points among different groups (GxT2-GxT1). Significant differences were found in FLD and FBS ($p < .05$), but not in FBT and FBM ($p > .05$; Table 7).

Table 8 compares the absolute discrepancies between post-extraction of group 1 and pre-extraction of all groups (G1T2-GxT1). Significant differences were found in FLD, FBS and FBT ($p < .05$), but not in FBM ($p > .05$; Table 8).

Table 9 compares the absolute discrepancies between pre-extraction of group 1 and pre-extraction of all other groups (G1T1-GxT1). Significant differences were found in FLD, FBS and FBT ($p < .05$), but not in FBM ($p > .05$; Table 9).

Table 10 compares the absolute discrepancies between post-extraction of group 1 and post-extraction of all other groups (G1T2-GxT2). Significant differences were found in FLD, FBS and FBT ($p < .05$), but not in FBM ($p > .05$; Table 10).

The percentage frequency distribution of coordinates that were affected by the reduced clarity and identified with professional judgment is illustrated in Table 11 and Figure 8. The percentage of affected coordinates increases as the resolution decreases. FLD and FBM identifications were most affected when tooth was present and absent respectively (Table 11 and Figure 8).

Table 7: Comparison of absolute discrepancies before and after tooth extraction among different CBCT settings (Groups) using Friedman's Two-Way Analysis of Variance by Ranks and Wilcoxon Signed Rank Tests with Bonferroni adjustment for pairwise comparison at $\alpha = 0.05$.

	Absolute discrepancies of paired GxT2-GxT1				
	Mean ± SD in mm				
Parameter	G1T2-G1T1	G2T2-G2T1	G3T2-G3T1	G4T2-G4T1	p-value
Facial Lamina Dura	0.09 ± 0.11^{a}	$0.09 \pm 0.09^{a,b}$	$0.12 \pm 0.11^{a,b}$	0.13 ± 0.11^{b}	.001*
Facial Bone Surface	0.06 ± 0.09^{a}	$0.08 \pm 0.08^{a,b}$	0.11 ± 0.11^{b}	0.11 ± 0.11^{b}	.002*
Facial Bone Thickness	0.10 ± 0.11	0.10 ± 0.10	0.14 ± 0.15	0.13 ± 0.12	.109
Facial Bone Margin	0.12 ± 0.18	0.17 ± 0.21	0.24 ± 0.24	0.18 ± 0.22	.087

*Statistically significant difference. [a,b]Different letters denote statistically significant difference.

Table 8: Comparison of absolute discrepancies from G1T2 paired with pre-extraction combinations (GxT1) using Friedman's Two-Way Analysis of Variance by Ranks and Wilcoxon Signed Rank Tests with Bonferroni adjustment for pairwise comparison at $\alpha = 0.05$.

	Absolute discrepancies of paired G1T2-GxT1				
	Mean ± SD in mm				
Parameter	G1T2-G1T1	G1T2-G2T1	G1T2-G3T1	G1T2-G4T1	p-value
Facial Lamina Dura	0.09 ± 0.11^{a}	0.12 ± 0.12^{a}	0.14 ± 0.12^{b}	0.17 ± 0.13^{b}	<.001*
Facial Bone Surface	0.06 ± 0.09^{a}	0.08 ± 0.09^{a}	$0.10 \pm 0.09^{a,b}$	0.13 ± 0.11^{b}	<.001*
Facial Bone Thickness	0.10 ± 0.11^{a}	0.11 ± 0.13^{a}	$0.13 \pm 0.12^{a,b}$	0.16 ± 0.14^{b}	.003*
Facial Bone Margin	0.12 ± 0.18	0.12 ± 0.09	0.18 ± 0.21	0.14 ± 0.17	.503

*Statistically significant difference. [a,b]Different letters denote statistically significant difference.

Table 9: Comparison of absolute discrepancies from the G1T1 combination paired with pre-extraction combinations (GxT1) using Friedman's Two-Way Analysis of Variance by Ranks and Wilcoxon Signed Rank Tests with Bonferroni adjustment for pairwise comparison at $\alpha = 0.05$.

	Absolute discrepancies of paired G1T1-GxT1			
	Mean ± SD in mm			
Parameter	G1T1-G2T1	G1T1-G3T1	G1T1-G4T1	p-value
Facial Lamina Dura	0.06 ± 0.07^{a}	0.09 ± 0.09^{a}	0.13 ± 0.11^{b}	<.001*
Facial Bone Surface	0.05 ± 0.07^{a}	$0.07 \pm 0.09^{a,b}$	0.10 ± 0.12^{b}	.002*
Facial Bone Thickness	0.06 ± 0.08^{a}	0.10 ± 0.09^{b}	0.16 ± 0.15^{b}	<.001*
Facial Bone Margin	0.08 ± 0.10	0.16 ± 0.34	0.16 ± 0.33	.486

*Statistically significant difference. [a,b]Different letters denote statistically significant difference.

Table 10: Comparison of absolute discrepancies from the G1T2 combination paired with post-extraction combinations (GxT2) using Friedman's Two-Way Analysis of Variance by Ranks and Wilcoxon Signed Rank Tests with Bonferroni adjustment for pairwise comparison at $\alpha = 0.05$.

	Absolute discrepancies of paired G1T2-GxT2			
	Mean ± SD in mm			
Parameter	G1T2-G2T2	G1T2-G3T2	G1T2-G4T2	p-value
Facial Lamina Dura	0.05 ± 0.06^{a}	$0.08 \pm 0.07^{a,b}$	0.10 ± 0.10^{b}	<.001*
Facial Bone Surface	0.06 ± 0.07^{a}	$0.08 \pm 0.07^{a,b}$	0.11 ± 0.09^{b}	<.001*
Facial Bone Thickness	0.08 ± 0.08^{a}	0.09 ± 0.08^{a}	0.16 ± 0.12^{b}	<.001*
Facial Bone Margin	0.13 ± 0.10	0.14 ± 0.11	0.19 ± 0.15	.321

*Statistically significant difference. [a,b]Different letters denote statistically significant difference.

Table 11. Percentage frequency distribution of coordinates that were affected by reduced clarity and had to be identified with professional judgment.

GxTy Combination	Percentage frequency distribution of coordinates requiring professional judgment		
	FLD	FBS	FBM
G1T1	14.6	0	0
G1T2	0	0	0
G2T1	32.3	2.1	0
G2T2	0	0	0
G3T1	52.1	0	8.3
G3T2	3.1	0	0
G4T1	76.0	9.4	37.5
G4T2	5.2	2.1	29.2

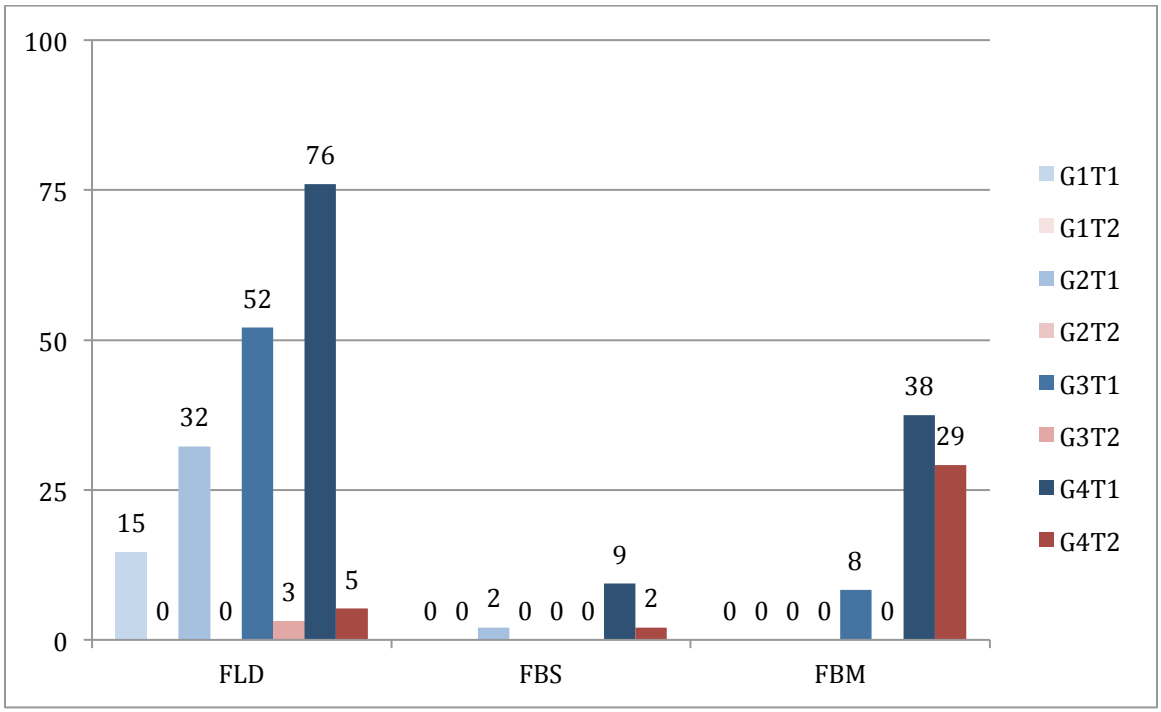

Figure 8. Percentage frequency distribution of coordinates that were affected by the reduced clarity and identified with professional judgment. Shades of blue represent the pre-extraction combinations and shades of red represent the post-extraction combinations.

Discussion

Image production with CBCT is an exceptionally sophisticated process with a multitude of factors influencing the final outcome.[9] These include, but are not limited to the scanning unit employed, FOV, voxel size, tissue density, and scan duration.[9] The research demonstrating accuracy of linear measurement with CBCT is abundant.[9,10-13] Spatial resolution, when evaluating fine anatomical structures however, is not as well understood.[5,9]

Image acquisition with detail that accurately reflects the clinical truth is important for practitioners to make sound diagnostic decisions and assess treatment outcomes.[3,4,14] Small anatomical structures, like the buccal bone is of particular interest.[3,4,14] This study sought to investigate what effect changing the voxel size and FOV, both before and after extractions, had on the ability to interpret the outline of the buccal bone.

Even though the results of this study were reported in both directional and absolute values, only absolute values were used for statistical analysis. This is because absolute values better reflect magnitudes of any discrepancies between paired groups, whereas directional data tend to mitigate them.

Of a total of 52 coordinate discrepancies, only 15 (7 for FLD, 3 for FBS, 5 for FBT and none for FBM) demonstrated significant differences (Tables 3-6). The mean absolute discrepancies between the coordinates that were statistically significantly different ranged from 0.08-0.17 mm (Tables 3-5). These discrepancies are small and probably clinically inconsequential. Furthermore, all paired coordinates were highly correlated ($r \geq .883$, $P < .001$; Tables 3-6). These results indicate that the ability to identify the boundaries of the buccal bone, irrespective of the presence of the tooth, is not

clinically significantly affected by the variation in FOV and voxel size of the CBCT images.

Beyond the direct coordinate comparison, evaluating how the coordinate discrepancies compared to each other had statistically significant results (Tables 7-10). Measuring how the magnitudes of discrepancies change with different parameter settings or with the presence or absence of a tooth reveals the importance of each of these variables. Table 7 makes discrepancy comparisons between pre- and post-extraction among all groups and shows the effects of tooth presence with alteration of scanning parameters. Table 8 makes discrepancy comparisons between G1T2 (highest resolution setting without a tooth present) to all groups pre-extraction, which shows how tooth presence and alteration of scanning parameters relate to the highest possible resolution imagery. Table 9 makes discrepancy comparisons among all groups with the teeth present, which reveals the effect from only changing scanning parameters with the teeth retained. Lastly, Table 10 makes discrepancy comparisons among all groups with the teeth extracted; this shows the effect from only changing scanning parameters without the potentially influential presence of the adjacent, similarly radiodense teeth.

Discrepancies for identifying the FBM showed no statistically significant differences for any comparison (Tables 7-10). For the remaining parameters (FLD, FBS, FBT), there is a trend evident in the discrepancy comparisons. The T1-T2 coordinate discrepancies between paired lower resolution images were larger in magnitude than the discrepancies between paired higher resolution images. For instance, looking at FBS, the G4T2-G4T1 discrepancy measured 0.11 ± 0.11mm, whereas the G1T2-G1T1 discrepancy calculated to be 0.06 ± 0.09mm (significantly different, Table 7). Additionally, the

coordinate discrepancies of a comparison between a higher resolution image to a lower resolution image are statistically significantly larger than coordinate discrepancies of a comparison between two higher resolution images. For example, with the FLD, the G1T2-G4T1 discrepancy calculated to be 0.17 ± 0.13mm, whereas the G1T2-G1T1 discrepancy calculated to be 0.09 ± 0.11mm (significantly different, Table 8). This remains true with the discrepancy comparisons in Tables 9 and 10, in which discrepancy comparisons between groups are made with and without the presence of the teeth, respectively. The trend here is intuitive; that lower resolution images can lead to greater discrepancies in interpretation than higher resolution images. However, the magnitudes of these discrepancies were small enough to be determined clinically negligible.

The results from this study corroborate the findings of several other authors.[14-17] The salient principle that can be gleaned from these investigations is that scanning parameters yielding lower resolution examinations maintain adequate diagnostic quality for identification of buccal bone during routine orthodontic evaluation.

When plotting the coordinates, some of the points were not well delineated; as in, no clear outline existed between the boundary of the buccal bone and the adjacent structure, either air or cementum. Identifying these coordinates required a professional judgment, or "best educated guess". The points where this was true were recorded and the frequency and proportions of these data were illustrated in Table 11 and Figure 8. The frequency of these unclear boundaries increases inversely with the spatial resolution of the image. The highest proportion of unclear coordinates involved the FLD parameter with the presence of adjacent teeth (T1). In the G4T1 combination, 76% of plotted points required an educated guess to identify. At times, the PDL would appear entirely absent,

and the root structure would appear to blend into the alveolar bone. Very few points with bone boundaries adjacent to air required any speculation. This is presumably due to the obviously high contrast between air and bone. When this interface was unclear, the boundary of the bone was often obfuscated by soft tissue. This data was collected to help reveal the frequency of coordinates subjectively challenging to identify and substantiate the subjective appraisal of improvement in the higher resolution imagery.

Dosimetry related to CBCT is especially complicated and difficult to characterize.[8] Image acquisition and the associated radiation exposure is a complex and multifactorial process.[8] The many factors that contribute to the radiation exposure during any given CBCT include the often user adjustable settings of voxel size and FOV, scan duration, milliamperage, kilovolt potential, filtering, patient positioning, and the sensor technology and proprietary reconstruction algorithms used in the device itself.[1,8] As it specifically relates to the parameters investigated in this study, FOV and voxel size, radiation exposure is directly proportional to FOV and inversely proportional to voxel size.[8,17]

An increasingly popular method of reporting radiation dose to the patient is the technical quantification Dose-Area Product (DAP), represented by the unit $mGy.cm^2$, providing the dose level in the beam as well as the area irradiated.[18] This value is directly proportional to the oft-referenced and familiar effective dose with dosimetry studies. The NewTom 5G unit employed in this study calculates the DAP value for every examination performed. Table 12 outlines a representative sample of scan information from each parameter for one of the specimens used in this study. The DAP for the scans performed in this investigation appeared more dependent on the FOV than the voxel size; with

changes in the values only occurring to any significant degree with adjustment of the FOV (Table 12). With this knowledge, using the NewTom 5G, it would be advisable to prescribe the appropriate FOV and choose the smallest voxel size available to provide the highest clarity.

Table 12. Scan information from each parameter acquired from a single specimen (representative sample) used in the study.

NewTom 5G Scan Information				
FOV (cm x cm)	12x8	12x8	18x16	18x16
Voxel Size (μm)	100	150	150	300
Time (s)	5.4	5.4	3.6	3.6
mAs	69.6	69.8	13.0	13.0
DAP ($mGy.cm^2$)	1303	1307	901	900

Counter-intuitively, and contrary to the general trend,[8] the DAP decreased (lower radiation) with increased FOV in this investigation (Table 12). It can be speculated that this is due to the larger voxel size, reduced scanning duration, reduced mAs, and fewer basis images generated with the larger FOV. It is important to note that this outcome is specific to this individual unit and cannot be generalized to other CBCT instruments, as the image acquisition technique widely varies.

Pauwel et al identified that with consideration for the vast variety of elements contributing to the dosimetry of each examination, summarizing CBCT as a single entity is misguided.[8] Instead, the radiation dose from these devices can be viewed as a function of the parameters prescribed. Therefore, exposition parameters should be adjusted to meet the specific diagnostic needs of the patient and the clinical scenario.[8] Generally

speaking, higher resolution images require a larger amount of radiation to the subject.[6-8,14] As noted above, the underscored principle of any radiographic study is maximizing the clinical benefit for the patient while minimizing the risks of ionizing radiation. Especially regarding CBCT, with such a dramatic range of exposition, the value of higher resolution and clarity of an image must be judiciously balanced with that of radiation dose.[7,8]

The results from this study favor the use of parameters that mitigate the radiation exposure to the patient. The magnitudes of the differences in the ability to identify boundaries of fine anatomical structures, like the buccal bone, between high resolution and low resolution scans, as revealed in this data, do not justify the additional ionizing radiation for normal orthodontic purposes.

Conclusions

Higher CBCT image resolution usually incurs higher effective radiation doses. This study, with its own limitations, shows that the ability to accurately discern the boundaries of the facial bone enveloping a tooth, irrespective of the presence of the tooth structure, is not clinically significantly affected by the variation in FOV and voxel size of the CBCT images. For each CBCT machine utilized, clinicians should be aware of the settings that produce acceptable image clarity in the area of interest with the lowest effective dose and utilize them accordingly.

REFERENCES

1. Scarfe WC, Farman AG. What is cone-beam CT and how does it work? Dent Clin North Am 2008; 52:707–30.

2. Lamichane M, Anderson NK, Rigali PH, Seldin EB, Will LA. Accuracy of reconstructed images from cone-beam computed tomography scans. Am J Orthod Dentofacial Orthop 2009; 136(2):156.e1-e6.

3. Rungcharassaeng K, Caruso JM, Kan JY, Kim J, Taylor G. Factors affecting buccal bone changes of maxillary posterior teeth after rapid maxillary expansion. Am J Orthod Dentofacial Orthop 2007; 132:428.e1-8.

4. Roe P, Kan JYK, Rungcharassaeng K, Caruso JM, Zimmerman G, et al. Horizontal and vertical dimensional changes of peri-implant facial bone following immediate implant placement and provisionalization of maxillary anterior single implants: A 1-year cone beam computed tomography study. Int J Oral Maxillofac Implants 2012; 27:393-400.

5. Spin-Neto R, Gotfredsen E, Wenzel A. Impact of Voxel Size Variation on CBCT-Based Diagnostic Outcome in Dentistry: a Systematic Review. J Digit Imaging 2013; 26:813-20.

6. Ludlow JB, Walker C. Assessment of phantom dosimetry and image quality of i-CAT FLX cone-beam computed tomography. Am J Orthod Dentofacial Orthop 2013; 144:802-17.

7. Ludlow JB, Ivanovic M. Comparative dosimetry of dental CBCT devices and 64-slice CT for oral and maxillofacial radiology. Oral Surg Oral Med Oral Pathol Oral Radiol Endod 2008; 106:106-14.

8. Pauwels R, Beinsberger J, Collaert B, Theodorakou C, Rogers J, Walker A, et al. Effective doze range for dental cone beam computed tomography scanners. Eur J Radiol 2011; 81:267–71.

9. Molen AD. Considerations in the use of cone-beam computed tomography for buccal bone measurements. Am J Orthod Dentofacial Orthop 2010; 137:S130-135.

10. Kobayashi K, Shimoda S, Nakagawa Y, Yamamoto A. Accuracy in measurement of distance using limited cone-beam computerized tomography. Int J Oral Maxillofac Implants 2004; 19:228-31.

11. Lascala CA, Panella J, Marques MM. Analysis of the accuracy of linear measurements obtained by cone beam computed tomography (CBCT-NewTom). Dentomaxillofac Radiol 2004; 33:291-4.

12. Sun Z, Smith T, Kortam S, Kim DG, Tee BC, Fields H. Effect of bone thickness on alveolar bone-height measurements from cone-beam computed tomography images. Am J Orthod Dentofacial Orthop 2011;139:e117-27.

13. Patcas R, Muller L, Ullrich O, Peltomaki T. Accuracy of cone-beam computed tomography at different resolutions assessed on the bony covering of the mandibular anterior teeth. Am J Orthod Dentofacial Orthop 2012; 141: 41-50.

14. Cook VC, Timock AM, Crowe JJ, Wang M, Covell Jr DA. Accuracy of alveolar bone measurements from cone beam computed tomography acquired using varying settings. Orthod Craniofac Res 2015; 18(Suppl.1):127-36.

15. Damstra J, Fourie Z, Huddleston Slater JJ, Ren Y. Accuracy of linear measurements from cone-beam computed tomography-derived surface models of different voxel sizes. Am J Orthod Dentofacial Orthop 2010;137:16.e1-6.

16. Liedke GS, da Silveira HE, da Silveira HL, Dutra V, de Figueiredo JA. Influence of voxel size in the diagnostic ability of cone beam tomography to evaluate simulated external root resorption. J Endod 2009; 35:233–235.

17. Menezes CC, Janson G, Massaro CS, Cambiaghi L, Garib DG. Reproducibility of bone plate thickness measurements with Cone-Beam Computed Tomography using different image acquisition protocols. Dental Press J. Orthod 2010; 15(5):143-9.

18. Horner K, The SEDENTEXCT Project Consortium. Safety and Efficacy of a New and Emerging Dental X-ray Modality: SEDENTEXCT Project Final Report. www.sedentexct.eu. 2011.

19. Wood R, Sun Z, Chaudhry J, Ching Tee B, Kim D, Leblebicioglu B, England G. Factors affecting the accuracy of buccal alveolar bone height measurements from cone-beam computed tomography images. Am J Orthod Dentofacial Orthop 2013; 143:353-63.

20. Kwong JC, Palomo JM, Landers MA. Image quality produced by different cone-beam computed tomography settings. Am J Orthod Dentofacial Orthop 2008; 133:317-27.

21. Rottke D, Patzelt S, Poxleitner P, and Schulze D. Effective dose span of ten different cone beam CT devices. Dentomaxillofac Radiol 2013; 42: 20120417

22. Leung CC, Palomo L, Griffith R, Hans MG. Accuracy and reliability of cone-beam computed tomography for measuring alveolar bone height and detecting bony dehiscences and fenestrations. Am J Orthod Dentofacial Orthop 2010; 137(Suppl):S109-19.

23. Kamburoglu K, Murat S, Yuksel SP, Cebeci AR, Paksoy CS: Occlusal caries detection by using a cone-beam CT with different voxel resolutions and a digital intraoral sensor. Oral Surg Oral Med Oral Pathol Oral Radiol Endod 2010;109:63–69.

24. Kamburoglu K, Kursun S: A comparison of the diagnostic accuracy of CBCT images of different voxel resolutions used to detect simulated small internal resorption cavities. Int Endod J 2010;43:798–807.

25. Dalili Z, Taramsari M, Mousavi Mehr SZ, Salamat F: Diagnostic value of two modes of cone-beam computed tomography in evaluation of simulated external root resorption: an in vitro study. Imaging Sci Dent 2012;42:19–24.

26. Bauman R, Scarfe W, Clark S, Morelli J, Scheetz J, Farman A: Ex vivo detection of mesiobuccal canals in maxillary molars using CBCT at four different isotropic voxel dimensions. Int Endod J 2011; 44:752–758.

27. Maret D, et al: Effect of voxel size on accuracy of 3D reconstructions with cone beam CT. Dentomaxillofac Radiol 2012; 41:649–655.

28. De Vos W, Casselman J, Swennen GRJ. Cone-beam computerized tomography (CBCT) imaging of the oral and maxillofacial region: A systematic review of the literature. Int. J. Oral Maxillofac. Surg. 2009; 38: 609–625.

29. Stonecypher M. The Effect of Tooth Presence on Identification of Tooth Socket Lamina Dura Surface: a CBCT Study. Masters Thesis submitted to LLU Department of Orthodontics and Dentofacial Orthopedics. 2013.